The EMBO Journal (2012) 31, 1591–1604 | © 2012 European Molecular Biology Organization | All Rights Reserved 0261-4189/12
www.embojournal.org

THE EMBO JOURNAL

Cwc2 and its human homologue RBM22 promote an active conformation of the spliceosome catalytic centre

Nicolas Rasche[1], Olexandr Dybkov[1], Jana Schmitzová, Berktan Akyildiz, Patrizia Fabrizio and Reinhard Lührmann*

Department of Cellular Biochemistry, Max-Planck-Institute of Biophysical Chemistry, Göttingen, Germany

RNA-structural elements play key roles in pre-mRNA splicing catalysis; yet, the formation of catalytically competent RNA structures requires the assistance of spliceosomal proteins. We show that the *S. cerevisiae* Cwc2 protein functions prior to step 1 of splicing, and it is not required for the Prp2-mediated spliceosome remodelling that generates the catalytically active B* complex, suggesting that Cwc2 plays a more sophisticated role in the generation of a functional catalytic centre. In active spliceosomes, Cwc2 contacts catalytically important RNA elements, including the U6 internal stem-loop (ISL), and regions of U6 and the pre-mRNA intron near the 5′ splice site, placing Cwc2 at/near the spliceosome's catalytic centre. These interactions are evolutionarily conserved, as shown by studies with Cwc2's human counterpart RBM22, indicating that Cwc2/RBM22–RNA contacts are functionally important. We propose that Cwc2 induces an active conformation of the spliceosome's catalytic RNA elements. Thus, the function of RNA–RNA tertiary interactions within group II introns, namely to induce an active conformation of domain V, may be fulfilled by proteins that contact the functionally analogous U6-ISL, within the spliceosome.

The EMBO Journal (2012) **31,** 1591–1604. doi:10.1038/emboj.2011.502; Published online 13 January 2012
Subject Categories: RNA
Keywords: catalytic centre; Cwc2; RBM22; spliceosome; U6-ISL

Introduction

Pre-mRNA splicing proceeds via two phosphoester transfer reactions and is catalysed by the spliceosome, which consists of the U1, U2, U4/U6 and U5 snRNPs and numerous proteins (Jurica and Moore, 2003; Will and Lührmann, 2011). During spliceosome assembly, short conserved sequences of the pre-mRNA, including the 5′ and 3′ splice sites (SSs) and the branch site (BS) are recognized in turn. Initially, U1 and U2 snRNPs bind, forming the A complex; this is followed by the U4/U6.U5 tri-snRNP, generating the B complex, which however does not yet have an active site. For catalytic activation, the spliceosome undergoes major structural and compositional rearrangements, which are driven by several RNA helicases. Initially, U1 and U4 snRNAs are displaced by the concerted action of the RNA helicases Prp28 and Brr2 (Staley and Guthrie, 1998), giving rise to the activated spliceosome or B^{act} complex. At the protein level, all U1 and U4/U6 snRNP proteins are also displaced, while at the same time numerous proteins are stably integrated into the B^{act} complex, as demonstrated by recent mass-spectrometric (MS) analysis of various spliceosomal complexes (Fabrizio *et al*, 2009). The B^{act} complex is then converted into the catalytically activated B* complex by the action of the Prp2 RNA helicase and its co-activator Spp2 (Kim and Lin, 1996; Warkocki *et al*, 2009). Following the recruitment of the splicing factor Cwc25 (Chiu *et al*, 2009; Warkocki *et al*, 2009), the first step of splicing occurs, whereby the 5′ SS of the pre-mRNA is cleaved and the 5′ end of the intron is ligated to the BS adenosine to form a lariat-like structure; concomitantly the C complex is formed. Subsequently, the C complex is remodelled, a process driven by the RNA helicase Prp16, which leads to rearrangements at the catalytic centre required for exon ligation and also to assist with splicing fidelity (Burgess and Guthrie, 1993; Konarska *et al*, 2006; Query and Konarska, 2006; Mefford and Staley, 2009). Following exon ligation and release of the mRNP from the spliceosome, the intron lariat spliceosome is disassembled and the snRNPs are thought to reassemble for a new round of splicing.

A complex RNA–RNA network involving the snRNAs and the pre-mRNA is formed during spliceosome assembly, and the resulting RNA structure plays a central role in catalysing the two steps of splicing (Nilsen, 1998; Valadkhan, 2005). Initially, U1 and U2 RNA base pair with the 5′ SS and BS, respectively. Within the tri-snRNP, U4 and U6 are extensively base paired. During integration of the tri-snRNP into the spliceosome, the U5 RNA initially contacts nucleotides (nts) of the 5′ exon near the 5′ SS and later also the 3′ exon (Sontheimer and Steitz, 1993; O'Keefe and Newman, 1998). In the preactivated spliceosome, the 3′ end of U6 RNA base pairs with the 5′ end of the U2 RNA to form the U2/U6 helix II (Wu and Manley, 1991; Madhani and Guthrie, 1994; Xu and Friesen, 2001).

During spliceosome activation, the U1/5′ SS and the U4/U6 base pairing interactions are disrupted and the U1 and U4 RNAs dissociate from the spliceosome. At the same time, U6 RNA rearranges and forms an internal stem-loop (ISL) that plays a central role in the catalysis of splicing (Fortner *et al*, 1994). The U6-ISL contains an internal bulge region (including U80 in yeast) that is critical for metal-ion binding and contains additional functionally important residues (Yean

*Corresponding author. Department of Cellular Biochemistry, Max-Planck-Institute of Biophysical Chemistry, Am Fassberg 11, Göttingen 37077, Germany. Tel.: +49 551 201 1405; Fax: +49 551 201 1197; E-mail: reinhard.luehrmann@mpi-bpc.mpg.de
[1]These authors contributed equally to the work

Received: 12 August 2011; accepted: 15 December 2011; published online: 13 January 2012

et al, 2000; Huppler *et al*, 2002; McManus *et al*, 2007). U6 RNA also forms additional base pairs with U2 generating U2/U6 helix I, which is composed of two short helices, Ia and Ib, separated by a 2-nt bulge in the U2 RNA (Madhani and Guthrie, 1992). Helix Ib contains the invariant AGC triad of U6 that has been suggested as binding a catalytic metal ion (Fabrizio and Abelson, 1992; Yean *et al*, 2000; Valadkhan and Manley, 2002; Butcher and Brow, 2005) and was shown to be essential for splicing (Fabrizio and Abelson, 1990; Hilliker and Staley, 2004). Finally, U6 RNA via its conserved ACAGAGA sequence also forms base pairs with the 5′ end of the intron (Kandels-Lewis and Séraphin, 1993; Lesser and Guthrie, 1993). In this arrangement, the BS is juxtaposed with the 5′ SS. While the importance of individual RNA-structural elements such as U6-ISL, U2/U6 helix I and the U6-ACAGAGA/5′ SS helix for splicing catalysis has received strong experimental confirmation, little is known about how these various RNA elements are brought into a catalytically active tertiary conformation. This appears to be of utmost importance, if one considers the manner in which the catalytic centre of the group II self-splicing introns is organized (Toor *et al*, 2008). A number of similarities between pre-mRNA and group II intron splicing make it plausible that the RNA elements of the respective catalytic core adopt similar folds in both systems. These include (i) the identical chemistry of the catalytic steps of both kinds of splicing and (ii) the great similarity between catalytically important structural elements in group II introns and the spliceosomal RNA network, especially between domain V (DV) of group II introns (which forms a stem-loop) and the U6-ISL, both of which bind catalytically active metal ions (Yean *et al*, 2000; Toor *et al*, 2008; Michel *et al*, 2009; Keating *et al*, 2010). One of the most impressive features revealed by the recently published crystal structure of an intact self-spliced group IIC intron is how numerous long-distance interactions between conserved structural elements of DI to VI and DV are essential to induce an unusual, catalytically important fold in DV (Toor *et al*, 2008).

In view of the apparent paucity of conserved RNA tertiary structures in spliceosomal introns that might direct the folding and juxtaposition of essential catalytic RNA-structural elements—such as the U6-ISL and helix Ib—into an active conformation, it seems likely that spliceosomal proteins may have taken over this function, at least in part. Prp8, a major scaffolding protein of the spliceosome, which contacts all of the chemically reactive sites of the pre-mRNA intron, would be an ideal candidate for this task (Grainger and Beggs, 2005). Other candidates would be one or more of those proteins that become stably integrated into the spliceosome during its activation (i.e., the formation of the B^{act} complex). In yeast, these include (i) a protein complex termed the 'nineteen complex' (NTC) that consists of eight core proteins (Prp19, Cef1, Snt309, Syf1, Syf2, Clf1, Isy1, and Ntc20) (Tarn *et al*, 1994; Chen *et al*, 2001; Hogg *et al*, 2010) and (ii) an additional set of at least 12 proteins (Ecm2, Cwc2, Cwc15, Bud31, Yju2, Prp17, Cwc21, Cwc22, Cwc24, Cwc27, Prp45, and Prp46) (Fabrizio *et al*, 2009). For simplicity, the latter group will henceforth be termed 'NTC-related proteins', because several of them have been shown to interact loosely with one or more of the NTC core proteins (Ohi and Gould, 2002; Vander Kooi *et al*, 2010).

The NTC plays an important role in regulating spliceosome conformation and fidelity, and it is required for promoting stable interactions of U5 and U6 RNAs with the pre-mRNA during activation of the spliceosome (Chan *et al*, 2003; Chan and Cheng, 2005). Whether the NTC proteins are directly involved in specifying new RNA interactions and/or conformations during splicing, or whether they achieve this indirectly, by recruiting NTC-related proteins that interact with the spliceosome's RNA network, is poorly understood. Consistent with the latter, several NTC-related proteins possess putative RNA-binding domains or have been shown to display strong genetic interactions with mutations in the catalytic RNA interaction network (Hogg *et al*, 2010). Among these, the yeast Cwc2 protein is of particular interest, in that it (i) has an RNA-recognition motif (RRM) and zinc-finger domains, (ii) is essential for pre-mRNA splicing *in vivo*, and (iii) has been shown to contact U6 RNA during splicing in yeast extracts (McGrail *et al*, 2009).

Here, we show that Cwc2 is essential for step 1 of splicing *in vitro*, and that it is not required for the Prp2-mediated remodelling step that generates the catalytically competent B* complex. We demonstrate that in purified catalytically active spliceosomes, Cwc2 contacts the U6-ISL, as well as regions of the U6 RNA and the intron adjacent to the 5′ SS. Chemical structure probing further suggests that Cwc2 may also directly or indirectly contact U6/U2 helix I. Thus, our data place Cwc2 at the heart of the spliceosome's catalytic centre. We subsequently show that RNA interactions involving Cwc2 are evolutionarily conserved, as demonstrated by studies of its human counterpart RBM22, indicating that the observed Cwc2/RBM22 RNA contacts in the spliceosome are functionally important. We propose that Cwc2, in co-operation with Prp8, induces an active conformation of the catalytic RNA elements in the spliceosome. Our data thus suggest that the function of RNA–RNA tertiary interactions within group II introns, namely to induce a catalytically active RNA conformation of DV, has potentially been taken over by proteins that contact the functionally analogous U6-ISL, within the spliceosome.

Results

Cwc2 is essential for step 1 of splicing in vitro

To gain a better understanding of the role of Cwc2 in pre-mRNA splicing, we performed splicing with standard yeast splicing extracts depleted of Cwc2 (ΔCwc2). Depletion was achieved by using a yeast strain (SC1887) that expresses Cwc2 tagged with the Tandem Affinity Purification (TAP) tag at its C terminus (Puig *et al*, 2001). Extracts were incubated with Sepharose beads that carried IgG (to which the TAP tag binds efficiently), or—as a 'mock depletion' control—with similar beads lacking IgG. Western blotting demonstrated that Cwc2 was removed efficiently (Figure 1A, lane 3).

Yeast extracts depleted of Cwc2 were then assayed for their ability to splice actin pre-mRNA. While the control and mock-depleted extracts spliced pre-mRNA efficiently, no splicing intermediates or products were observed with the ΔCwc2 extract (Figure 1B, lanes 1–9). However, when ΔCwc2 extracts were complemented with recombinant Cwc2, splicing of actin pre-mRNA was restored to a level similar to that observed with the control extracts (lanes 10–12). These data demonstrate that Cwc2 is required for step 1 of pre-mRNA splicing. Moreover, they show that depletion of endogenous Cwc2 from yeast splicing extracts does not result in signifi-

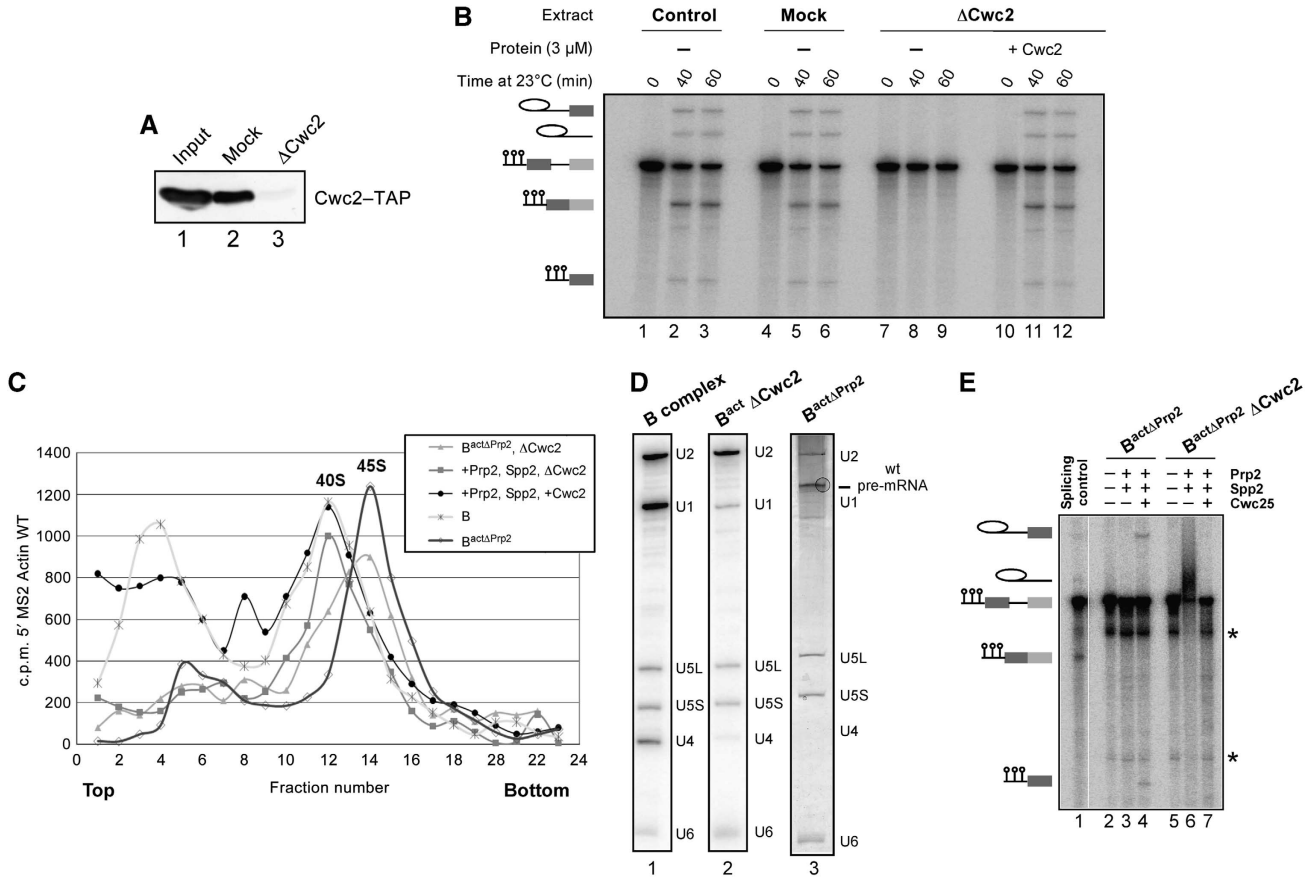

Figure 1 Cwc2 is essential for step 1 of splicing *in vitro* and it is not required for the Prp2-mediated remodelling step. (**A**) Western blot analysis of yeast splicing extracts carrying Cwc2 tagged with the TAP tag before (lanes 1 and 2) and after depletion of Cwc2 (lane 3). (**B**) A uniformly ^{32}P-labelled M3Act pre-mRNA was incubated in yeast whole-cell extract (lanes 1–3), which was either mock- (lanes 4–6) or Cwc2-depleted (lanes 7–12), under standard splicing conditions. Recombinant Cwc2 was then added to a final concentration of 3 μM (lanes 10–12). The splicing mixtures were incubated at 23°C and stopped at the time indicated. RNA was analysed on an 8% urea–polyacrylamide gel and visualized by autoradiography. The positions of the pre-mRNAs, the splicing intermediates, and products are indicated on the left. (**C**) Profiles of affinity-purified $B^{actΔPrp2}$ spliceosomes depleted of Cwc2 ($B^{actΔPrp2}$ ΔCwc2), after incubation with Prp2/Spp2/ATP (+Prp2, Spp2 ΔCwc2) and Prp2/Spp2/ATP plus recombinant Cwc2 (+Prp2, Spp2 +Cwc2). Profiles of affinity-purified $B^{act\ ΔPrp2}$ spliceosomes before depletion of Cwc2 ($B^{actΔPrp2}$) and of affinity-purified B complexes are also shown. Spliceosomes were separated on a glycerol gradient containing 75 mM KCl. The radioactivity contained in each gradient fraction was determined by Cherenkov counting. Sedimentation coefficients were determined by comparison with the UV absorbance profile of a reference gradient containing prokaryotic ribosomal subunits. (**D**) RNAs isolated from the B and the ΔCwc2 B^{act} complex (lanes 1 and 2) were visualized by northern blot analysis. Lane 3, RNAs isolated from complex $B^{actΔPrp2}$ (visualized by silver staining). RNA identities are indicated on the right. (**E**) Affinity-purified Cwc2 mock-depleted $B^{actΔPrp2}$ spliceosomes (lane 4) and ΔCwc2 $B^{actΔPrp2}$ spliceosomes were incubated with Prp2, Spp2, ATP, and Cwc25 for 45 min at 23°C (lane 7). Asterisks: uncharacterized pre-mRNA-derived bands.

cant co-depletion of one or more other proteins required for pre-mRNA splicing.

Cwc2 is not required for the activation of the spliceosome or for its remodelling by Prp2

We previously showed that Cwc2 is recruited to the spliceosome during its activation step, i.e., during the transition from complex B to B^{act}, when U1 and U4 snRNAs are dissociated. We therefore investigated whether Cwc2 is required for this transition. To monitor the transition, we exploited the fact that complex B has a Svedberg (S) value of 40, while complex B^{act} to which it is transformed has an S value of 45 (see also Figure 1C and Fabrizio *et al*, 2009).

We used a yeast strain that contains a temperature-sensitive Prp2 helicase (*prp2-1*) and also expresses Cwc2 with a C-terminal TAP tag (strain YNR1). Splicing extracts of these cells were depleted of endogenous Cwc2 (see above), and the mutated Prp2 was then inactivated by 30 min incubation at 35°C. Splicing was initiated by adding ^{32}P-labelled actin pre-mRNA that carried three MS2 RNA aptamers at its 5′ end (M3Act pre-mRNA) and the splicing reaction was further incubated for 50 min at 23°C. The resulting spliceosomal complexes were affinity purified via MS2–MBP-based chromatography (Fabrizio *et al*, 2009; Warkocki *et al*, 2009) and examined by analytical ultracentrifugation in a glycerol gradient. Figure 1C shows that most of the purified complex ΔCwc2 $B^{actΔPrp2}$ had an S value of about 45. A parallel experiment using Cwc2 mock-depleted splicing extracts, but otherwise identical to the first, gave a very similar result (Figure 1C, $B^{actΔPrp2}$).

These results imply that the transition from complex B (40S) to B^{act} (45S) took place, so that Cwc2 is not required for this process. This inference is supported by an RNA analysis of the isolated spliceosomal complexes (Figure 1D): while 40S B complexes contain, as expected, all of the snRNPs U1, U2, U4, U5 and U6 in similar molar quantities (lane 1), the

45S spliceosomal complexes assembled in ΔCwc2 splicing extracts show only small quantities of U1 and U4 snRNAs, while U2, U5 and U6 RNAs are represented in quantities similarly to those found in the B complex, confirming the identity of the 45S particles as B^{act} (lane 2 compare with lane 3). These results further show that Cwc2, apart from being not needed for the activation of the spliceosome, is also not needed for the stable integration of the U5 and U6 snRNAs into the spliceosome during the B to B^{act} transition. Thus, Cwc2 clearly has a function distinct from that of the core NTC complex.

It was previously shown that Prp2 triggers a major remodelling of the activated spliceosome in an ATP-dependent step as a prerequisite for catalytic activation of the spliceosome (i.e., transition from the B^{act} to B* complex). This remodelling step results in a decrease in the S value of the spliceosome from 45S (B^{act}) to 40S (B*), a process which also involves the destabilization of the interaction of the U2 SF3a and SF3b proteins (Kim and Lin, 1996; Warkocki *et al*, 2009). To investigate whether Cwc2 is involved in this Prp2-mediated remodelling step, we incubated affinity-purified 45S ΔCwc2 $B^{actΔPrp2}$ spliceosomes with Prp2, Spp2, and ATP for 30 min at 23°C and then analysed their sedimentation behaviour in a glycerol gradient. Figure 1C shows that the majority of these spliceosomes now sediment with an S value of ~40S (+Prp2, +Spp2, ΔCwc2). Thus, efficient ATP-dependent Prp2 remodelling of the spliceosome can also occur in the absence of Cwc2. While the Prp2-remodelled ΔCwc2 B^{act} complex (+Prp2, +Spp2, ΔCwc2) exhibits a similar S value as a wild-type B* complex, it is catalytically inactive. This was shown by the following experiment (Figure 1E). We have incubated affinity-purified 45S ΔCwc2 $B^{actΔPrp2}$ spliceosomes with Prp2, Spp2, ATP, and Cwc25 for 45 min at 23°C (lane 7). As a control, we have carried out the same experiment except that purified 45S $B^{actΔPrp2}$ spliceosomes were Cwc2 mock depleted (lane 4). Only the Cwc2 containing spliceosomes were capable of carrying out catalytic step 1 of splicing (lane 4), while ΔCwc2 B^{act} spliceosomes were catalytically inactive (lane 7), despite the fact that they can undergo the Prp2 mediated remodelling step.

Cwc2 can be crosslinked to U6 RNA and the pre-mRNA in activated spliceosomes

The results described above demonstrate that Cwc2 is needed for step 1 of splicing but its absence does not lead to a major spliceosome assembly defect. This suggests that Cwc2 plays a more sophisticated role in the generation of the functional catalytic centre of the spliceosome. We therefore next investigated whether Cwc2 interacts with the spliceosomal RNAs during the activation and catalytic phases of the spliceosomal cycle by performing UV irradiation of purified spliceosomes, which induces zero-length protein–RNA crosslinks. Using yeast splicing extracts that contained TAP-tagged Cwc2, we assembled B^{act} and C complexes on the ^{32}P-labelled pre-mRNA constructs M3ActΔ6 and M3ActΔ31, respectively, that are truncated downstream of the BS and were previously used to isolate these complexes (Fabrizio *et al*, 2009). B* complexes were likewise assembled on ^{32}P-labelled wild-type actin pre-mRNA using splicing extracts derived from the *prp2-1* strain which expressed a TAP-tagged Cwc2 protein; in this case, before the assembly step, the extract was incubated for 30 min at 35°C to inactivate the endogenous Prp2. In each case, the spliceosomal complexes formed were affinity purified, UV irradiated for 1 min and then subjected to denaturing conditions in order to disrupt protein–protein and non-covalent RNA–protein interactions. An aliquot was retained, and the remainder of the sample was incubated with IgG Sepharose, allowing the selective immunoprecipitation of RNA species crosslinked to Cwc2-TAP. After proteolytic digestion, co-precipitated snRNAs were identified by northern blotting using probes that hybridize to U2, U5, and U6 RNAs.

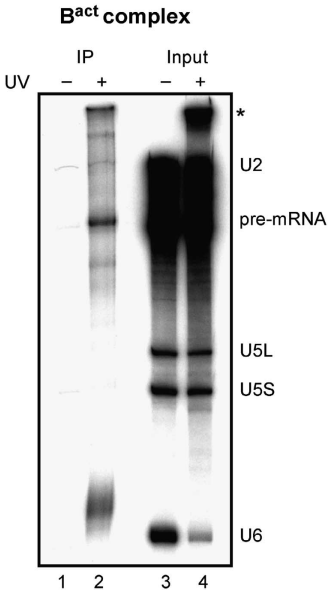

Figure 2 Cwc2 crosslinks to yeast U6 RNA and pre-mRNA within activated spliceosomes. Northern analysis of the snRNA derived from UV-irradiated B^{act} complexes carrying Cwc2 tagged with the TAP tag (lane 4) and after immunoprecipitation of B^{act} complexes with IgG Sepharose beads (IP, lane 2). Lanes 1 and 3 are controls without UV irradiation. RNA was analysed on an 8% polyacrylamide gel and visualized by autoradiography. The positions of the snRNAs and M3ActΔ6 pre-mRNA are indicated on the right. Asterisk: high-molecular weight crosslinked product.

As an example, results for purified B^{act} complexes are presented in Figure 2 (note that the ^{32}P-labelled pre-mRNA used for complex formation is also visible in the autoradiogram). Upon UV irradiation of the purified B^{act} complexes some loss of U6 RNA was observed, while the other RNA signals remained largely unchanged (Figure 2, compare lanes 3 and 4). In the absence of UV irradiation, no RNA was co-immunoprecipitated together with Cwc2 (lane 1), confirming that all non-covalent RNA–protein interactions were disrupted under the immunoprecipitation conditions used. In contrast, upon UV irradiation solely the U6 RNA and the pre-mRNA were co-precipitated. The crosslinked U6 RNA migrated more slowly than unmodified U6 RNA, presumably due to a bound residual oligopeptide (digestion fragment) of Cwc2. These data indicate that in the purified B^{act} complex, Cwc2 can be crosslinked specifically to U6 RNA and to the pre-mRNA. Similar results were obtained upon UV irradiation of purified B* and C complexes, indicating that Cwc2 directly contacts the U6 RNA and pre-mRNA in the yeast spliceosome during its activation and catalytic phases (see the more detailed analysis below).

Previously, it was shown that the U5 snRNP proteins Prp8 and Snu114 could be crosslinked to U6 RNA in yeast

U4/U6.U5 tri-snRNPs (Vidal *et al*, 1999). To investigate whether these proteins would crosslink to U6 RNA also in the B^{act} spliceosome, we carried out the same crosslinking experiments as described above for Cwc2, using extracts from yeast strains that expressed TAP-tagged U5 proteins Prp8 or Snu114, or the TAP-tagged NTC-related proteins Ecm2 or Yju2 (as additional controls), for the assembly of B^{act} complexes on the ^{32}P-labelled pre-mRNA construct M3ActΔ6. Importantly, while these proteins could be crosslinked to pre-mRNA (Prp8, Snu114, Ecm2) or U5 RNA (Prp8, Snu114), or U2 RNA (Snu114), none of them was found to crosslink to U6 RNA (Supplementary Figure S1), demonstrating a very selective crosslinking behaviour of the five proteins tested here (including Cwc2). To further exclude the possibility that our Cwc2–U6 RNA crosslinked species are partly due to other, simultaneously crosslinked proteins we performed an additional control experiment. After UV irradiation of the purified B^{act} complex, we disrupted it by treatment with a detergent and pulled down specifically the U6 RNA by using a complementary oligonucleotide immobilized on Sepharose beads. The protein(s) associated with the U6 RNA attached to the beads were digested with trypsin and analysed by MS; this revealed that Cwc2 solely crosslinked to U6 RNA in the B^{act} complex. Thus, any additional protein possibly crosslinked simultaneously with Cwc2 to U6 RNA was undetectable by MS under our conditions.

Cwc2 interacts with the U6-ISL and a region upstream of the U6 ACAGAGA box

Next, we mapped the crosslinking sites of Cwc2 on the U6 RNA and pre-mRNA. Thus, we performed primer-extension analysis of the U6 RNA in purified B^{act}, B*, and C complexes (Ehresmann *et al*, 1987; Figure 3A–C), and also of the actin pre-mRNA in the B^{act} complex (Figure 3D). Putative RNA–protein contact sites were determined by comparing the patterns of reverse transcription stops. Reverse transcriptase (RT) cannot read through the nucleotides covalently attached to an amino acid or peptide by UV irradiation and thus stops after transcribing the nucleotide immediately preceding it (Ehresmann *et al*, 1987). In all three complexes, a strong RT stop was observed at U6 nucleotide G39 (located just upstream of the U6 ACAGAGA box), four weaker stops at nucleotides U65–C68 (in the stem of the U6-ISL), and one at U74 (in the loop of the U6-ISL). All of them were dependent on UV irradiation of spliceosomes (lanes 6–9 in Figure 3A–C) and were not observed after UV irradiation of *in-vitro* transcribed U6 RNA (Figure 3A, lanes 10 and 11). All of these spliceosome-dependent RT stops were observed exclusively when crosslinked TAP-Cwc2-RNA species were specifically precipitated with IgG Sepharose under denaturing conditions, indicating that the protein contacting these nucleotides in native B^{act} complexes was indeed Cwc2 (lanes 6 and 7, Figure 3A).

While the crosslink with G39 appeared to be equally strong in all three complexes, there were differences in the intensity of the weaker stops. In the C complex, significant stops were observed at nucleotides U65, C68, and U74 but not at nucleotides C66 and C67, while in complex B* the stops at nucleotides U65, C68, and U74 were less intense than in complex C. These minor differences observed in crosslinks in the loop and stem of the U6-ISL, suggest changes in the interaction between Cwc2 and the ISL during the catalytic phase of the spliceosome cycle, which could in turn suggest the possibility of conformational changes in the ISL at this stage of splicing.

To obtain additional, independent experimental evidence that the crosslinks detected to the U6-ISL in the C complex were due to Cwc2 and not to a different protein, the purified crosslinked TAP–Cwc2–U6 RNA species was specifically cut into two by oligo-directed RNaseH cleavage using a DNA oligonucleotide that hybridized to nucleotides 42–61 of U6 RNA. The sample was incubated with IgG Sepharose, allowing the selective immunoprecipitation of the 5′ and/or the 3′ portion of U6 RNA (e.g., containing the U6-ISL) crosslinked to Cwc2-TAP. Co-precipitated RNAs were identified by northern blotting using a probe that hybridizes to U6 RNA. This experiment showed that both portions of U6 RNA were precipitated, thereby demonstrating that the crosslinking sites detected in the U6-ISL at the stage of C complex were due to Cwc2 (unpublished data). The signals from nucleotides C85 to A90 were seen in the RNP samples (lanes 7 and 9) and also in UV irradiated *in-vitro* transcribed U6 RNA (lane 11), indicating that these were RT stops due to RNA–RNA crosslinks between adjacent nucleotides or, alternatively, even strand cleavage.

The corresponding analysis of the pre-mRNA intron in the B^{act} complex (Figure 3D) revealed crosslinks between Cwc2 and U222 of the pre-mRNA, the latter corresponding to uridine +15 of the intron. These observations are summarized in Figure 3E for complexes B^{act} and C, in the context of the U6/U2/pre-mRNA interaction network proposed for the catalytic centre. The existence of crosslinks between Cwc2 and U6 G39, on the one hand, and between Cwc2 and U+15 of the pre-mRNA intron, on the other hand, suggests that these two nucleotides simultaneously contact Cwc2, and thus are in close proximity in the spliceosome. As Cwc2 also contacts the ISL, one possible function of Cwc2 might be to orient and/or juxtapose the ISL region of U6 RNA and the ACAGAGA/5′ SS RNA element (see Discussion).

Structure probing of native and Cwc2-depleted B^{act} complexes

UV crosslinking provides important clues about the contacts between a protein and an RNA, but only restricted information about the rest of their interaction surface. In the B^{act} complex, the latter issue is especially important, as here the crosslinks between Cwc2 and nucleotides of the U6-ISL are relatively weak compared with those in complex C. We therefore performed chemical structure probing of U6 RNA with dimethylsulphate (DMS) and 1-cyclohexyl-3-(2-morpholinoethyl) carbodiimide metho-*p*-toluene sulphonate (CMCT) in purified, native B^{act} complexes versus B^{act} complexes assembled in ΔCwc2 splicing extracts (ΔCwc2 B^{act}). DMS modifies the Watson–Crick base pairing positions of adenosine and cytidine, while CMCT modifies uridine and, to a lesser extent, guanine (Moine *et al*, 1997). Under the buffer conditions used here, we observed that CMCT also modifies to some extent cytidine and adenosine residues. Modified bases were detected by primer-extension analyses (Figure 4A). In the native B^{act} complex, only a few nucleotides of the U6 RNA were highly accessible to DMS and CMCT. These were primarily in the loop of the 5′ stem-loop (i.e., A12 and C14), the nucleotides around A26 and A62, which connects U6/U2 helix Ib with the U6-ISL. Importantly,

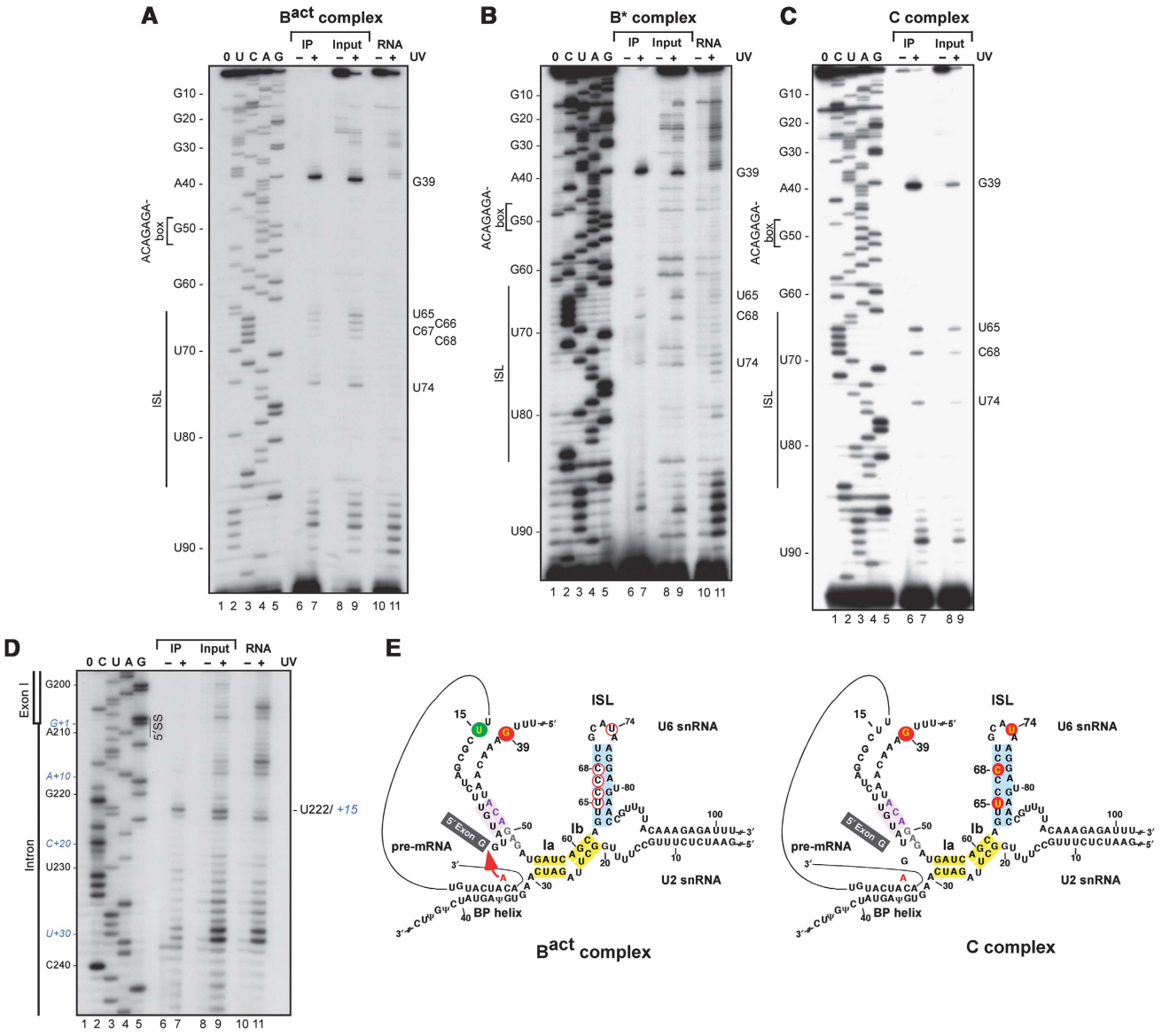

Figure 3 Cwc2 interacts with the U6-ISL and a region upstream of the ACAGAGA box. (**A**–**C**) Primer-extension analysis of U6 RNA derived from UV-irradiated B^{act}, B*, and C complexes, respectively, containing TAP-tagged Cwc2, after immunoprecipitation with IgG Sepharose beads (IP, lane 7), or without immunoprecipitation (input, lane 9). Lane 11, analysis of UV-irradiated *in-vitro* transcribed U6 RNA, lanes 6, 8, and 10 are controls without UV irradiation. U, C, A, and G are dideoxy sequence markers ('0', no ddNTP). Regions corresponding to the U6-ACAGAGA and ISL sequences are marked on the left. Reverse-transcriptase stops that are due to RNA–protein crosslinks are denoted on the right. (**D**) Primer-extension analysis of M3ActΔ6 pre-mRNA derived from UV-irradiated B^{act} complex, after immunoprecipitation with IgG resin (IP, lane 7) or without immunoprecipitation (input, lane 9). Analysis of UV-irradiated M3ActΔ6 RNA prepared by transcription *in vitro* (lane 11). The primer used was complementary to positions 254–269 of yeast M3ActΔ6 pre-mRNA. The reverse-transcriptase stop that is due to an RNA–Cwc2 crosslink is denoted on the right. (**E**) Secondary-structure models of U2/U6/pre-mRNA before (B^{act} complex) and after (C complex) step 1 of splicing according to Madhani and Guthrie (1992). The attack of the BS A at the 5′ SS is indicated by an arrow in the B^{act} complex. Sites in U6 crosslinked to Cwc2 are indicated by red circles, open circles indicate weak, and closed circles indicate strong crosslinks, respectively. Green circle: site in the pre-mRNA intron crosslinked to Cwc2.

nucleotides flanking G39 and the loop of the U6-ISL, where Cwc2 crosslinks were mapped, are poorly or not at all accessible (lane 5 in both panels; see Supplementary Figure S2 for a quantitative analysis of U6 nucleotide accessibilities). In contrast, in ΔCwc2 B^{act} complexes, these regions were clearly accessible to DMS and CMCT (lanes 5 and 7 in both panels). This suggests that Cwc2 interacts with several additional nucleotides surrounding the crosslink sites at G39 upstream of the ACAGAGA box and U74 of the U6-ISL loop in the native B^{act} complex. A slight increase in accessibility in the absence of Cwc2 was also observed for the nucleotides between U64 and U70, i.e., the 'left' side of the U6-ISL stem, while nucleotides of the complementary strand were not accessible in either complex (see Figure 4B for a summary of the U6 RNA sequences that are protected in the presence of Cwc2). The only exception is U80, which is more accessible in ΔCwc2 B^{act} complexes. Additional U6 nucleotides that are more accessible in ΔCwc2 B^{act} compared with the native B^{act} complex include several nucleotides within or flanking the ACAGAGA box such as U46, A51, U54 and nucleotides U88–U91 downstream of the U6-ISL. Importantly, the modification pattern of U6 RNA in B^{act} complexes purified from

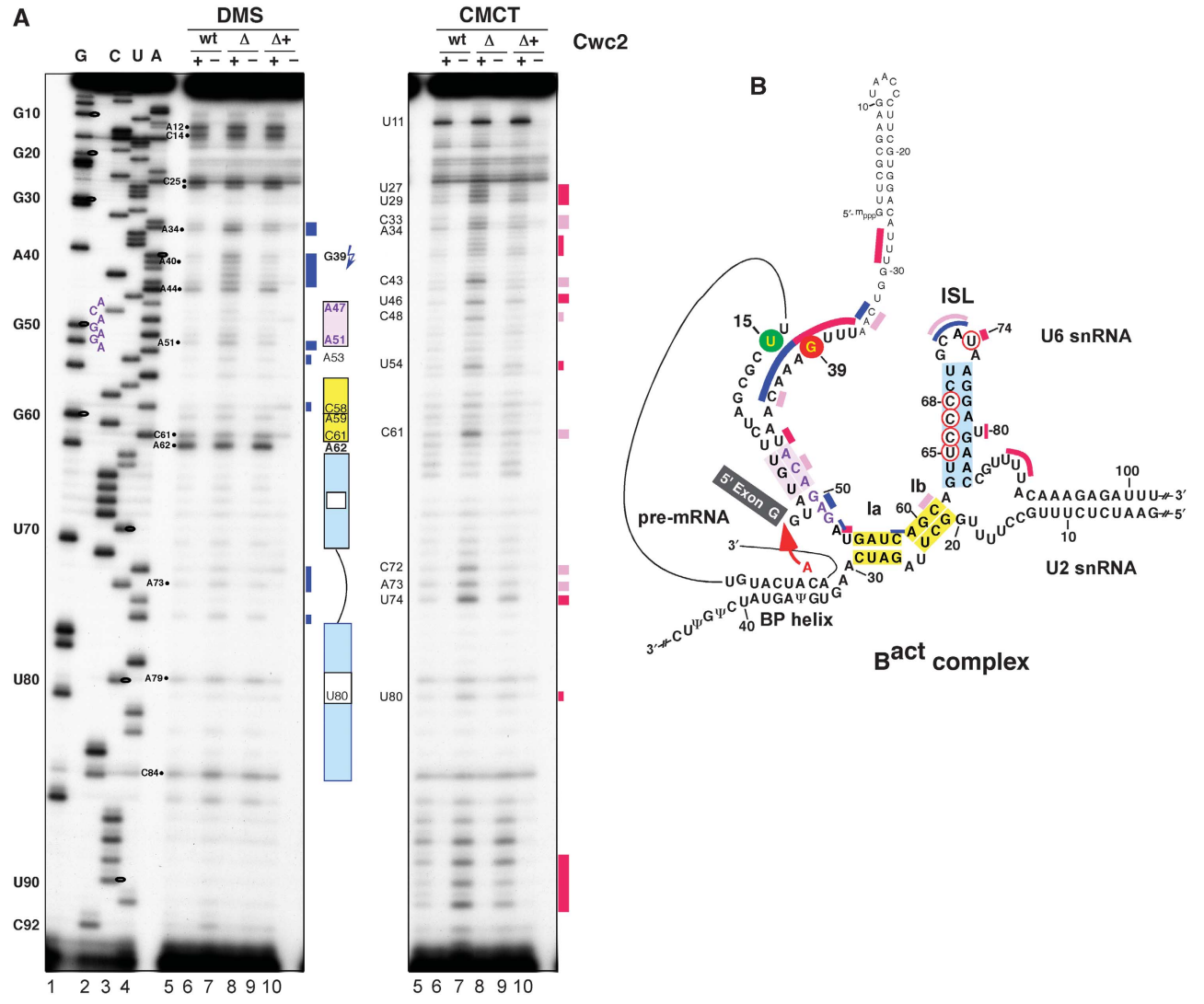

Figure 4 Structure probing in native and ΔCwc2 B^{act} complexes. (**A**) Structure probing with DMS and CMCT. Lanes 5 and 6 (wt) 'wild-type' B^{act} complex, lanes 7 and 8 (Δ) B^{act} complex assembled in ΔCwc2 extract, and lanes 9 and 10 (Δ+) B^{act} complex assembled in ΔCwc2 supplemented with 1 μM recombinant Cwc2. In lanes 5, 7, and 9 ('+'), the reaction mixture was complete, while in lanes 6, 8, and 10 ('−'), the chemical reagent was omitted. G, C, U, A are sequencing ladders. The arrow indicates the U6 G39 nucleotide crosslinked to Cwc2. The positions of protected nucleotides in native purified complexes are shown on the right with blue stripes for DMS and red stripes for CMCT. Pink stripes indicate cytidine and adenosine residues unusually modified by CMCT. (**B**) Secondary-structure model of U2/U6/pre-mRNA before step 1 of splicing. The attack of the BS A at the 5′ SS is indicated by an arrow. Bases in U6 protected from modification towards DMS and CMCT, respectively, in the presence of Cwc2, are represented by blue, red, and pink stripes superimposed on the secondary-structure models of the U6 RNA. Red and green circles are described in the legend of Figure 3.

Cwc2-depleted splicing extract then complemented with recombinant Cwc2 prior to spliceosome assembly resembles closely the one observed with native purified B^{act} complexes (compare lane 9 with lanes 5 and 7 in both panels and see Supplementary Figure S2). This is particularly true for the regions around G39, the ACAGAGA box, the left strand of the ISL and the ISL loop.

The combined data of our UV crosslinking and structure probing experiment indicated that in the B^{act} complex Cwc2 interacts with the region upstream of the ACAGAGA box around G39 and with the ISL of U6 RNA. The increased accessibility towards DMS and CMCT of the ACAGAGA box region in the absence of Cwc2 is consistent with the idea that Cwc2 may also interact with this area. However, in the absence of a Cwc2-ACAGAGA box crosslink, we cannot exclude the possibility that one or more additional proteins may contact the ACAGAGA box and that their recruitment to this site could be dependent on the presence of Cwc2.

RBM22, the human homologue of yeast Cwc2, is required for pre-mRNA splicing in vitro

We have shown that Cwc2 interacts with the U6 ISL and upstream of the ACAGAGA box during the activation and catalytic phases of the spliceosomal cycle in yeast. As Cwc2 is essential for step 1 of splicing in yeast (Figure 1), it is highly likely that its interaction with U6 (and potentially also the pre-mRNA) is a prerequisite for step 1. If such a centrally positioned RNA–protein interaction is indeed of functional importance, it should be highly conserved through evolution. We thus next focussed on the apparent human homologue of Cwc2, namely RBM22 (McGrail *et al*, 2009). A sequence comparison of yCwc2 with hRBM22 reveals that the middle

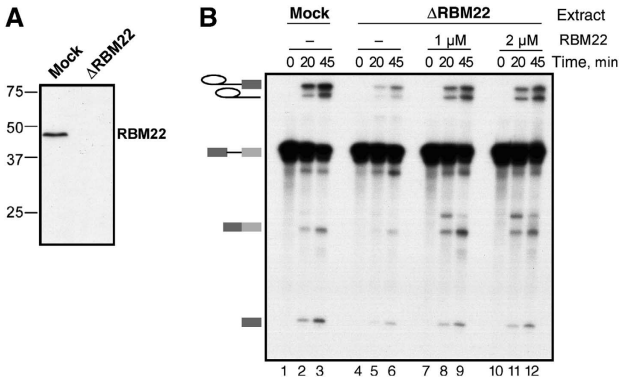

Figure 5 RBM22, the human homologue of yeast Cwc2, is required for pre-mRNA splicing *in vitro*. (**A**) Western blot analysis of HeLa nuclear extracts before (mock) and after depletion of RBM22 (ΔRBM22). (**B**) A uniformly ^{32}P-labelled MINX pre-mRNA was incubated in mock-depleted (lanes 1–3) or RBM22-depleted (lanes 4–12) HeLa nuclear extract, under standard splicing conditions. Recombinant RBM22 was added to a final concentration of 1 μM (lanes 7–9) or 2 μM (lanes 10–12). The splicing reactions were stopped at the times indicated. RNA was analysed on a 14% polyacrylamide gel and visualized by autoradiography. The residual splicing activity of the ΔRBM22 extract was 15% of that of the mock-depleted extract (lane 5 versus lane 2).

part of RBM22, comprising the RRM and the zinc finger, is significantly conserved (39% similarity, 26% identity: Supplementary Figure S3). Interestingly, the N-terminal region of RBM22 also shows homology with the N-terminal part of another yeast protein, Ecm2 (51% similarity and 37% identity). In fact, RBM22 is the only human protein that shares homology with both yeast Cwc2 and Ecm2 (see Discussion).

We first investigated whether RBM22 is important for pre-mRNA splicing *in vitro*. Therefore, we raised antibodies against a peptide of RBM22 and, using them, we were able to immunodeplete RBM22 efficiently from HeLa nuclear extracts (Figure 5A). We then performed *in vitro* splicing with a uniformly ^{32}P-labelled MINX pre-mRNA and either mock-depleted or RBM22-depleted extract (ΔRBM22). A significant decrease in both the splicing intermediates and products was observed in the ΔRBM22 extract as compared with the mock-depleted extract (Figure 5B, compare lanes 3 and 6). Significantly, addition of recombinant RBM22 to the ΔRBM22 extract reversed the observed splicing defect (compare lanes 4–6 with lanes 7–9 and 10–12). These results indicate that RBM22 is required for step 1 of splicing. As our supply of antibodies was limited, we were unable to determine at what stage of spliceosome assembly (e.g., B or B^{act} complex) splicing was blocked in the ΔRBM22 extract.

RBM22 interacts with U6 RNA and the pre-mRNA in human B^{act} and C complexes

Next, we investigated via UV crosslinking whether RBM22 also interacts with U6 RNA and the pre-mRNA in the human spliceosome as observed for Cwc2 in yeast. We recently showed that in HeLa splicing extracts a B^{act} complex can be assembled on a pre-mRNA construct containing a short 20 nt-long polypyrimidine tract after the BS (PM5–20 construct) (Bessonov *et al*, 2010). This complex lacks U1 and U4 snRNPs but contains stoichiometric amounts of human NTC proteins and NTC-related proteins including RBM22 (Agafonov *et al*, 2011). A PM5 construct containing a long polypyrimidine tract, but lacking the 3′ SS and the downstream exon, allows the efficient formation of human C complexes (Bessonov *et al*, 2008). It is currently not possible to stall the assembly of the human spliceosome at the stage of the B* complex.

We affinity purified human B^{act} and C complexes assembled on the aforementioned pre-mRNA substrates, subjected them to UV irradiation, and immunoprecipitated crosslinked RBM22–RNA species under denaturing conditions, as described above for the yeast system. Co-immunoprecipitated snRNAs were analysed by northern blotting. The signal from U6 RNA in the input lane of irradiated B^{act} complexes is strongly reduced compared with non-irradiated complexes, and a relatively indistinct, diffuse signal appears slightly below the U5 band (Figure 6A, lanes 1 and 2). In the αRBM22–RNA immunoprecipitate, only one RNA band appears, and this can be assigned unambiguously to U6 RNA, as shown in the lower panel, which was obtained after hybridization with an anti-U6 probe only (lane 3). The slower migration of the crosslinked U6 RNA indicates that, in spite of protease digestion, a relatively large protein fragment remains attached to the RNA. Similar results were obtained with UV-irradiated C complexes (lanes 5–8); whereby the yield of the crosslink between RBM22 and U6 appeared greater than that observed with B^{act} complexes.

We also investigated whether RBM22 is crosslinked to the ^{32}P-labelled pre-mRNA present in the human B^{act} and C complexes. Upon irradiation of B^{act} complexes, the pre-mRNA migrated slightly slower in the gel (Figure 6B, lane 1). Pre-mRNA was co-immunoprecipitated together with RBM22 (lane 3), demonstrating that a pre-mRNA-RBM22 crosslink is formed. With the C complex, the splicing intermediates, i.e., exon 1 and intron lariat (exon 2 is lacking in the PM5 pre-mRNA), and low levels of contaminating pre-mRNA are seen (lanes 5 and 6). Pre-mRNA and the lariat intermediate (but not exon 1) were co-immunoprecipitated with RBM22 (lane 7). Thus, in the human C complex, RBM22 is crosslinked only to the intron lariat, indicating that it contacts the intron during the first catalytic step of the spliceosome.

RBM22 interacts with U6 RNA at sites equivalent to those contacted by Cwc2 in yeast spliceosomes

To identify RBM22 crosslink sites on the U6 RNA and the pre-mRNA in B^{act} and C complexes, we carried out primer-extension analyses, as described above for yeast. With the B^{act} complex, several UV-dependent reverse transcription stops (e.g., nucleotides 24–26, 34, 52, 62, and 66–68) were detected, which were not, or only to a minor extent, observed in the irradiated RNA-only control (Figure 7A, compare lane 9 with 11); thus, these stops are likely due to protein–RNA crosslinks. Indeed, several of these stops were also observed after immunoprecipitation with anti-RBM22 antibodies (lane 7). As the stops at nucleotides U32 and U52 were also observed in the UV-irradiated RNA-only control, they probably represent RNA–RNA crosslinks. The other stops at nucleotides A24, C25, U26, G34, C66 and a weak one at C62, were not observed in the UV-irradiated RNA control and therefore represent RBM22–U6 RNA crosslinks (lane 7). Thus, similarly to Cwc2 in yeast spliceosomes, RBM22 can be crosslinked efficiently to nucleotides upstream of the ACAGAGA box of U6 RNA and weakly to the upper part of U6-ISL (Figure 7C). Similar results were obtained with

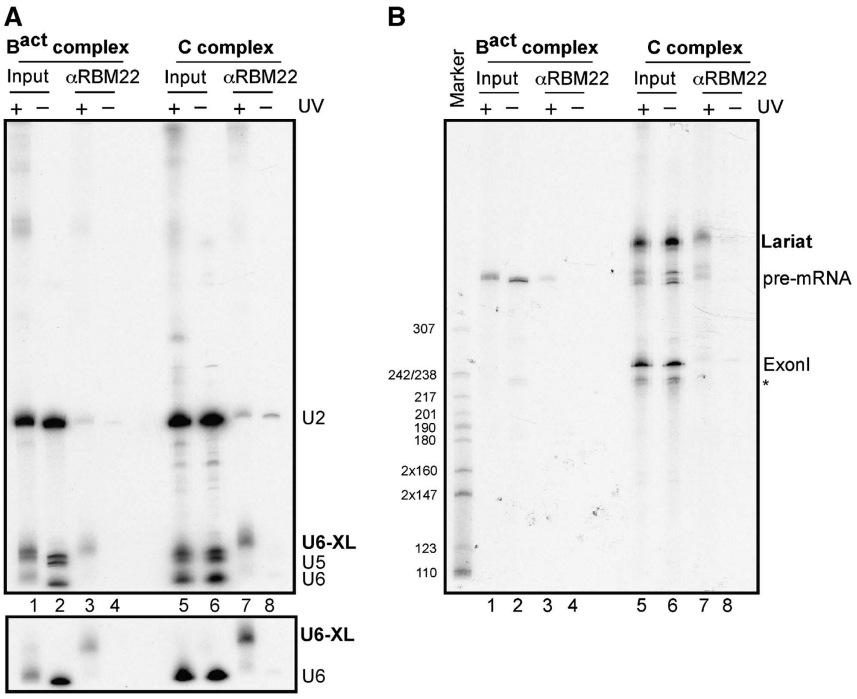

Figure 6 RBM22 interacts with the U6 RNA and pre-mRNA in human B^{act} and C complexes. (**A**) Northern analysis of the snRNA derived from UV-irradiated B^{act} and C complexes, after immunoprecipitation with anti-RBM22 antibody (αRBM22, lanes 3 and 7) or without immunoprecipitation (input, lanes 1 and 5). Lanes 2, 4 and 3, 8 are controls without UV irradiation. RNA was visualized by autoradiography after hybridization with probes complementary to human U2, U5, and U6 RNAs (upper panel) or to U6 RNA only (lower panel). (**B**) Analysis of ^{32}P-labelled PM5 pre-mRNA derived from UV-irradiated human B^{act} and C complexes, after immunoprecipitation with anti-RBM22 antibody (αRBM22, lanes 3 and 7) or without immunoprecipitation (input, lanes 1 and 5). RNA was analysed on a 10% polyacrylamide gel. The positions of the pre-mRNAs and the splicing intermediates are indicated on the right. Asterisk: degradation product of the pre-mRNA derived from oligo-directed Rnase H digestion during preparation of the C complex.

UV-irradiated C complexes (Figure 7B), except that the yield of the Cwc2 crosslink to C62 located in the upper part of the U6-ISL stem was significantly greater than in the B^{act} -complex. Thus, U6–RBM22 contacts are also maintained during step 1 of splicing.

Finally, we performed primer-extension analysis using an oligonucleotide complementary to the pre-mRNA intron (Supplementary Figure S4A and B). Inspection of the RT stops in human B^{act} and C complexes after immunoprecipitation with the anti-RBM22 antibodies revealed that RBM22 crosslinks to nucleotides 268–270 of the pre-mRNA, corresponding to nucleotides +26 to +28 of the intron (Supplementary Figure S4A and B). Thus, RBM22 also contacts intron nucleotides downstream of the 5′ SS. In summary, RBM22 interacts with both the U6 RNA and the pre-mRNA in the human spliceosome similarly to its yeast counterpart Cwc2, and its interaction sites on the U6 RNA are conserved in both organisms. The evolutionarily highly conserved nature of these interactions strongly supports their functional importance during splicing.

Discussion

Cwc2 is essential for pre-mRNA splicing in vitro and it is not required for the Prp2-mediated remodelling of the activated spliceosome

Cwc2 is a member of the group of NTC-related proteins that, along with the core NTC complex, are stably integrated into the B^{act} complex during the activation of the spliceosome. Our results show that Cwc2 is essential for the formation of a catalytically competent spliceosome, but that it does not act until the late spliceosome maturation phase, just prior or during step 1. Depletion of Cwc2 from yeast splicing extracts leads to inhibition of splicing prior to step 1 (Figure 1). A B^{act}-like complex that (like a native B^{act} complex) has an S value of 45, no longer contains U1 or U4 snRNAs and possesses stably integrated U5 and U6 RNAs, is still assembled in the absence of Cwc2 (Figure 1D). This indicates that the core NTC complex can be integrated into the spliceosome in the absence of Cwc2, and thus that it is not needed for NTC recruitment to the B^{act} complex. Indeed, MS analyses of the isolated ΔCwc2 B^{act} complexes revealed that their protein composition, apart from the absence of Cwc2, is qualitatively identical to that of the native B^{act} complexes (unpublished data). In addition, we show that Cwc2 is not required for the Prp2/Spp2- and ATP-dependent remodelling of the B^{act} complex from a 45S to 40S spliceosomal complex (Figure 1C), a process that is accompanied by destabilization of the binding of the U2-SF3a and SF3b proteins (Warkocki *et al*, 2009). Cwc2 unlike other proteins, which dissociate after the first catalytic step, remains stably associated with the spliceosome during the entire catalytic phase. Due to its close association with the catalytic RNA network, it is likely that Cwc2 is required not only for step 1, but also for step 2 (see below).

Cwc2 interacts with catalytic RNA-structural elements in the spliceosome

A clue to a possible function of Cwc2 is provided by our UV RNA crosslinking and chemical structure probing experiments conducted with purified yeast spliceosomes in the

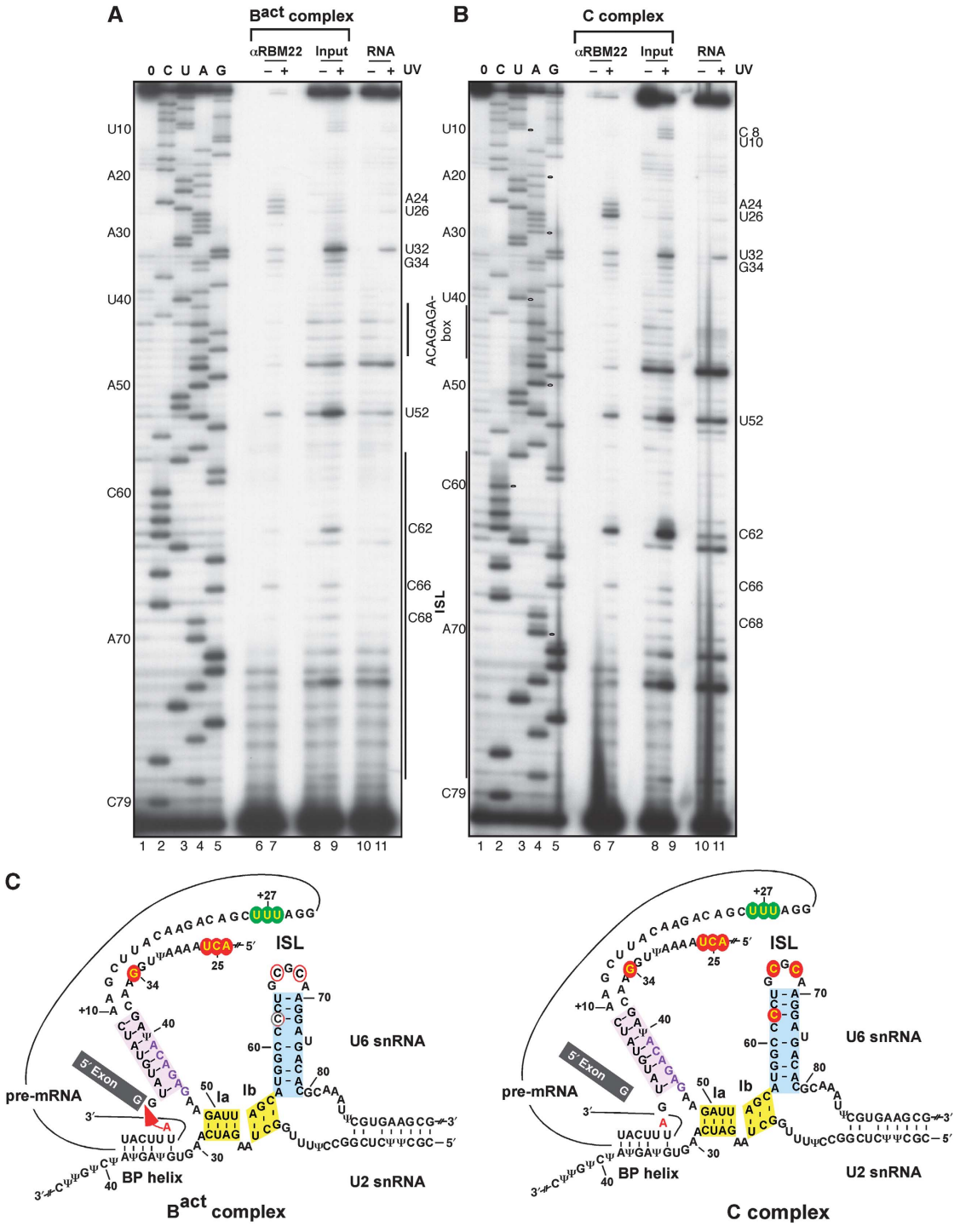

Figure 7 Mapping RBM22–U6 RNA and RBM22–pre-mRNA crosslinks. Primer-extension analysis of U6 RNA derived from UV-irradiated B^{act} (**A**) and C complexes (**B**), after immunoprecipitation with anti-RBM22 antibody (αRBM22, lane 7) or without immunoprecipitation (input, lane 9). Primer-extension analysis of UV-irradiated naked RNA isolated from B^{act} and C complexes, respectively (lane 11). Lanes 6, 8, and 10 are controls without UV irradiation. C, U, A and G are dideoxy sequence markers as above. Nucleotides within the U6 ACAGAGA and ISL sequences are marked by a bar to the right or left of each gel. Reverse-transcriptase stops that are due to RNA–protein crosslinks are denoted on the right. (**C**) Secondary-structure models of human U2/U6/pre-mRNA in the B^{act} and C complex, respectively. Sites in U6 and PM5 pre-mRNA (Supplementary Figure S4) crosslinked to RBM22 are as described for Cwc2 in the legend of Figure 3.

activation/catalytic phase (B^{act}, B*, and C). In all of these complexes, Cwc2 contacts two regions of the U6 RNA: nucleotides around G39, upstream of the ACAGAGA box, which is base paired with the 5′ SS, and the left part of the U6-ISL including the ISL loop (Figure 3).

It is instructive to examine the Cwc2–U6 RNA interactions in more detail and to compare them between the various spliceosomal complexes analysed. Crosslinking of Cwc2 to U6-G39 takes place already in complex B^{act}, with an efficiency equal to that observed with B* and C complexes

(Figure 3). Although only one nucleotide (G39) is crosslinked, Cwc2 probably contacts a longer stretch of the U6 RNA, both upstream and downstream of G39. This is suggested by the enhanced accessibility of the U6 RNA nucleotides C33–C43 towards chemical modifications in ΔCwc2 B^{act} compared with native B^{act} complexes (Figure 4). In contrast, the interaction of Cwc2 with the U6-ISL is more dynamic, in that the crosslinking pattern changes during the transition from B^{act} to B* to C (Figure 3). In the B^{act} complex, we observe only a low degree of crosslinking to U74 in the terminal loop and to U65–C68 on the 5′ side of the stem (Figure 3A). Nevertheless, Cwc2 appears to be in close contact with the ISL in the B^{act} complex, as shown by the enhanced accessibility of C72 and A73 towards chemical reagents in ΔCwc2 B^{act} complexes. Crosslinking of Cwc2 to the ISL is more pronounced in B* and especially in the C complex, in which the greatest degree of Cwc2 crosslinking is observed for U65 and C68 with little or no crosslinks formed with C66 and C67. This shift in crosslinking behaviour suggests that the conformation of the U6-ISL changes during the catalytic activation by Prp2/Spp2 and also during the transition to the post-step 1 spliceosome C complex. Taken together, our data indicate that one function of Cwc2 in the spliceosome could be to bring, or to help to keep, two functionally important RNA-structural elements close to one another, namely the ACAGAGA box/5′ SS element and the U6-ISL.

Interestingly, Cwc2 can also be crosslinked to a U at intron position +15 (relative to the 5′ SS), indicating that this region must be close to the G39-containing region of U6, upstream of the ACAGAGA box. By binding simultaneously to both of these single-stranded regions (U6 RNA and the intron), which are both close to the ACAGAGA/5′ SS element, Cwc2 could play a role in tethering this entire region to the U6-ISL. It is also possible that the simultaneous binding of Cwc2 to the U6-G39 and intron U+15 region reinforces or modulates the interaction between the ACAGAGA box and the 5′ SS. In this context, it is important to note that several nucleotides in and around the ACAGAGA box were found to be accessible to chemical reagents in the ΔCwc2 B^{act}, but not in the native B^{act} complex. The same is true for some U6 nucleotides in the U6/U2 helix I, especially for U6-C61 (Figure 4). This is consistent with the idea that Cwc2 also interacts with the ACAGAGA box/5′ SS and helix I. However, in the absence of Cwc2 crosslinks in these regions, we cannot exclude that one or more other proteins interact with these regions in a Cwc2-dependent manner. It is also possible that Cwc2 stabilizes a specific conformation of the active site of the spliceosome and that in the absence of Cwc2 the whole active site is destabilized or distorted, thus making the function of Cwc2 fundamental.

Recently, it was shown that the U6 ACAGAGA box is dynamically base paired with the 5′ SS, in a manner dependent upon the NTC complex (Chan and Cheng, 2005). As Cwc2 interacts with at least two proteins of the core NTC complex (Ohi and Gould, 2002), it is conceivable that NTC together with Cwc2 modulate the interaction between U6 RNA and the 5′ SS. In their RNA–RNA crosslinking study, the same authors noted that U6-G39 was crosslinked to an unidentified protein; it seems very likely that this is the Cwc2 crosslink that we describe here.

Evolutionary conservation of Cwc2 function in splicing

That the interaction between Cwc2 and spliceosomal catalytic RNA elements described here is of functional importance, is strongly supported by its striking evolutionary conservation. Like its yeast counterpart the human homologue of Cwc2, RBM22 (McGrail *et al*, 2009) is required for step 1 of splicing *in vitro* (Figure 5). In isolated human B^{act} and C complexes, RBM22 also is crosslinked to the corresponding regions of the human U6 RNA—i.e., the region upstream of the ACAGAGA box (G34 and A24–U26) and to nucleotides in the terminal loop of U6-ISL and to C62 in its stem. Furthermore, the differential yield of crosslinks between RBM22 and the U6-ISL in the B^{act} versus C complex is similar to what we detected in yeast spliceosomes (Figure 7). Moreover, RBM22 (like Cwc2) contacts intron nucleotides near the ACAGAGA/5′ SS box interaction site, although the crosslinks are located somewhat further downstream than in the yeast spliceosome. Thus, also in higher eukaryotes, this protein appears to aid in tethering of the ACAGAGA/5′ SS interaction elements to the U6-ISL. Close proximity between the ACAGAGA/5′ SS element and the U6-ISL, as indicated by our crosslinks between both of these regions and Cwc2/RBM22, is supported by previous site-directed hydroxyl-radical footprinting experiments with the BABE reagent placed at position +10 of the introns in human B^{act}/B* and C complexes. In both complexes, we detected cleavages not only 5′ of the ACAGAGA box, but also in the upper region of the U6-ISL (Rhode *et al*, 2006).

Contact between RNA and Cwc2/RBM22 in the spliceosome is consistent with the presence of two potential RNA-binding domains in both proteins—an RRM and a zinc finger—both of which are also conserved (Supplementary Figure S3; McGrail *et al*, 2009). Interestingly, RBM22 has an additional zinc finger-like sequence that, although absent in Cwc2, shows a clear sequence relationship with a zinc finger-like sequence in yeast Ecm2 (Xu and Friesen, 2001; Supplementary Figure S3). No other human spliceosomal protein exhibits significant homology with yeast Ecm2. This raises the interesting possibility that RBM22 might represent a fusion protein of yeasts Ecm2 and Cwc2, and thus functionally replace both proteins. Interestingly, Ecm2 was previously shown to play a role in the formation of the U2/U6 helix II during maturation of the spliceosome (Xu and Friesen, 2001).

Cwc2: a link between the RNA-catalytic centre and the protein network of the spliceosome

The multiple interactions between Cwc2 and the catalytic RNA network of the spliceosome together with its interactions with proteins of the core NTC complex such as Prp19 and Isy1 (Ohi and Gould, 2002) suggest that Cwc2 is an important link between the catalytic RNA network and factors that modulate the activity and the fidelity of the catalytic centre (Hogg *et al*, 2010). On the basis of elegant genetic studies, a two-state model of the spliceosome has recently been proposed in which the conformations required for the first and second steps are in thermodynamic equilibrium (Konarska and Query, 2005; Konarska *et al*, 2006). Interestingly, the two states can be stabilized/destabilized by various proteins and U6 RNA mutant alleles that affect the efficiency and fidelity of step 1 or step 2, respectively (Konarska and Query, 2005). How these conformational

changes are achieved at a molecular level is at present unclear. Due to the high degree of connectivity among spliceosomal proteins, local changes in the structure of the spliceosome—caused by certain protein or RNA mutations—could also be transmitted to the catalytic RNA network via Cwc2, thereby modulating the activity and/or fidelity of the catalytic centre. Consistent with this possibility is the observation that deletion of the NTC protein Isy1, which appears to interact with Cwc2 (Ohi and Gould, 2002), also influences the fidelity of step 1 (Villa and Guthrie, 2005).

A potential role for Cwc2/RBM22 in promoting an active conformation of the spliceosome's catalytic RNA elements

The recently published crystal structure of a self-splicing group IIC intron (Toor *et al*, 2008) revealed how the central element of the group II catalytic centre, stem-loop DV, is brought into a specific, catalytically active conformation by several long-range interactions. The upper and lower stems of DV are positioned at a 45° angle (relative to each other), which distorts the conformation of the bulge separating these stems and moves it into the vicinity of the catalytic RGC triad at the foot of the lower stem of DV (Keating *et al*, 2010; Toor *et al*, 2010). At the same time, the nucleotides of the catalytic triad form a catalytic triple helix together with C377 of the DV bulge and the J2/3 GC dinucleotides (GA in group IIA and B introns), bringing together catalytically essential residues of the introns (see Figures 2 and 7 in Keating *et al*, 2010).

In this constellation, the DV bulge and the triple helix together co-ordinate two Mg^{2+} ions in a configuration that is consistent with a two-metal-ion mechanism of splicing catalysis (Steitz and Steitz, 1993). An important feature of this is that formation of the catalytically active conformation of the DV stem-loop requires the entire group II intron structure.

The U6-ISL together with the U6/U2 helix Ib—which contains the catalytic U6-AGC triad—possesses all the biophysical properties of the DV element of group II introns and is a central, catalytically essential RNA element of the spliceosome (see above). This idea is supported strongly by the demonstration that, in the minor spliceosome, a group II intron DV stem-loop can replace the U6atac-ISL without loss of splicing activity (Shukla and Padgett, 2002). It has further been suggested that the catalytically important J2/3 GA dinucleotide may have a spliceosomal counterpart in the 3′-terminal GA of the U6 ACAGAGA box, which together with the U6-ISL bulge (U80 in yeast) could form a catalytic triplex with the AGC triad of the U6/U2 helix Ib (Keating *et al*, 2010). However, this would require that (i) the upper part of the ISL stem adopts a similarly angular, distorted conformation with respect to the bottom part and (ii) both the ACAGAGA box and the 5′ SS are positioned in proximity to helix Ib and the ISL. As there are no obviously conserved RNA elements in the spliceosome that, analogously to the situation in group II introns, could induce a catalytically active conformation of the U6-ISL, this task must at least partly be performed by proteins.

Our results indicate that Cwc2 is an ideal candidate for performing such a task. By tethering the partially base paired ACAGAGA/5′ SS element to the U6-ISL and by interacting either directly or indirectly with part of helix I and the ACAGAGA box (Figure 4), it could help promote formation of the putative catalytic triple helix discussed above. Moreover, by interacting with the terminal loop and the 5′ part of the stem of the U6-ISL, Cwc2 could potentially also promote an active conformation of the ISL. Thus, in the spliceosome, Cwc2 could, at least in part, substitute for the DI domain that in group II introns is responsible for inducing an active conformation of DV. However, whether the proposed catalytic triple helix (Toor *et al*, 2008; Keating *et al*, 2010) indeed forms in the spliceosome remains to be seen. Cwc2 could potentially even play a more active role in the creation of an active site by forming direct hydrogen bonds with nucleotides of the catalytic AGC triad in helix Ib and in this way replace one or more of the proposed base triplet interactions.

The observed interactions of Cwc2 with the catalytic RNA-structural elements of the spliceosome place Cwc2 at the heart of the catalytic centre. Another protein situated close to the active site of the spliceosome is Prp8 (Grainger and Beggs, 2005). Prp8 contacts all of the chemically reactive sites of the spliceosome, and it harbours an Rnase H-like domain in its C-terminal region (Pena *et al*, 2008; Ritchie *et al*, 2008; Yang *et al*, 2008), which helps to assemble and stabilize the spliceosome's catalytic core. As Prp8 and Cwc2 contact distinct regions of the catalytically important RNA elements of the spliceosome, the two proteins appear to cooperate in promoting a catalytically active conformation of the spliceosomal RNA–RNA interaction network (see above and Butcher and Brow, 2005). The essential nature of the collaboration between spliceosomal RNA elements and both Cwc2 and Prp8 in catalysing the splicing reaction, along with its evolutionary conservation, supports the idea that the spliceosome is an RNP enzyme containing active RNA rather than a ribozyme per se (Abelson, 2008).

Materials and methods

UV crosslinking of spliceosomes

Approximately 1–4 pmol of purified yeast complexes was pipetted onto pre-cooled 10-well multitest slides and then irradiated for 60 s with UV light at 254 nm on ice (Urlaub *et al*, 2002). To the irradiated and non-irradiated control samples of spliceosomal complexes, SDS was added to a final concentration of 1%, incubated for 10 min at 70°C and allowed to cool to room temperature before the addition of Triton X-100 to a final concentration of 5%. The samples were then diluted with 5–6 volumes of NET-150 buffer (50 mM Tris–HCl pH 7.4, 150 mM NaCl) and subjected to immunoprecipitation. Human complexes were UV irradiated for 30–40 s as above, ethanol precipitated and denatured in the 20 mM sodium phosphate buffer containing 130 mM NaCl and supplemented with 3% SDS. After heating, the samples were diluted with an equal volume of phosphate buffer supplemented with 10% Triton X-100. Prior to immunoprecipitation, the samples were diluted with eight volumes of phosphate buffer. In parallel, RNAs were gently extracted from spliceosomal complexes using phenol-chloroform extraction at 4°C to preserve the core RNA–RNA interactions. The RNA samples were crosslinked under the same conditions.

Immunoprecipitation of RNA–protein crosslinks

Protein A or IgG Sepharose (GE Healthcare) resins were washed with NET-150 buffer and incubated at 4°C with UV-crosslinked or non-crosslinked yeast or human spliceosomal complexes prepared as above. After washing with NET-150 buffer, beads were incubated with PK-mix (0.5–1 mg/ml Proteinase K, 50 mM EDTA pH 8.0, 1% SDS) for 20 min at 42°C followed by PCI extraction and ethanol precipitation. The pellet was dried and dissolved in water.

Primer-extension analysis

Oligodeoxynucleotide primers complementary to nucleotides 94–112 of the yeast U6, 254–269 of the M3Act pre-mRNA, 80–100 of human U6 RNA and 317–336 of PM5 pre-mRNA were labelled with ^{32}P at their 5′ end by T4 polynucleotide kinase, and $\sim 1–2 \times 10^5$ c.p.m. of primer was used for one reverse transcription reaction. The samples were denatured by heating at 96°C for 1 min, annealed by cooling to room temperature, and reverse transcribed with 1.5 U of AMV reverse transcriptase (USB) for 45 min at 43°C. Sequencing ladders were obtained from U6 RNA prepared by transcription *in vitro*, from M3Act or from PM5 pre-mRNAs under identical conditions, except that 0.05 mM dideoxynucleoside triphosphates were included. Reverse transcripts were separated on a 9.6% polyacrylamide sequencing gel containing 8.3 M urea and visualized by autoradiography.

Supplementary data

Supplementary data are available at *The EMBO Journal* Online (http://www.embojournal.org).

Acknowledgements

We thank Thomas Conrad for excellent technical assistance; Reinhard Rauhut for protein homology searches; Peter Odenwälder for help with spliceosomal complex purification and Cindy Will for constructive comments. This work was supported by a grant from the Deutsche Forschungsgemeinschaft SFB 860 to RL.

Conflict of interest

The authors declare that they have no conflict of interest.

References

Abelson J (2008) Is the spliceosome a ribonucleoprotein enzyme? *Nat Struct Mol Biol* **15:** 1235–1237

Agafonov DE, Deckert J, Wolf E, Odenwälder P, Bessonov S, Will CL, Urlaub H, Lührmann R (2011) Semiquantitative proteomic analysis of the human spliceosome via a novel two-dimensional gel electrophoresis method. *Mol Cell Biol* **31:** 2667–2682

Bessonov S, Anokhina M, Krasauskas A, Golas MM, Sander B, Will CL, Urlaub H, Stark H, Lührmann R (2010) Characterization of purified human Bact spliceosomal complexes reveals compositional and morphological changes during spliceosome activation and first step catalysis. *RNA* **16:** 2384–2403

Bessonov S, Anokhina M, Will CL, Urlaub H, Lührmann R (2008) Isolation of an active step I spliceosome and composition of its RNP core. *Nature* **452:** 846–850

Burgess SM, Guthrie C (1993) A mechanism to enhance mRNA splicing fidelity: the RNA-dependent ATPase Prp16 governs usage of a discard pathway for aberrant lariat intermediates. *Cell* **73:** 1377–1391

Butcher SE, Brow DA (2005) Towards understanding the catalytic core structure of the spliceosome. *Biochem Soc Trans* **33:** 447–449

Chan SP, Cheng SC (2005) The Prp19-associated complex is required for specifying interactions of U5 and U6 with Pre-mRNA during spliceosome activation. *J Biol Chem* **280:** 31190–31199

Chan SP, Kao DI, Tsai WY, Cheng SC (2003) The Prp19p-associated complex in spliceosome activation. *Science* **302:** 279–282

Chen CH, Tsai WY, Chen HR, Wang CH, Cheng SC (2001) Identification and characterization of two novel components of the Prp19p-associated complex, Ntc30p and Ntc20p. *J Biol Chem* **276:** 488–494

Chiu YF, Liu YC, Chiang TW, Yeh TC, Tseng CK, Wu NY, Cheng SC (2009) Cwc25 is a novel splicing factor required after Prp2 and Yju2 to facilitate the first catalytic reaction. *Mol Cell Biol* **29:** 5671–5678

Ehresmann C, Baudin F, Mougel M, Romby P, Ebel JP, Ehresmann B (1987) Probing the structure of RNAs in solution. *Nucleic Acids Res* **15:** 9109–9128

Fabrizio P, Abelson J (1990) Two domains of yeast U6 small nuclear RNA required for both steps of nuclear precursor messenger RNA splicing. *Science* **250:** 404–409

Fabrizio P, Abelson J (1992) Thiophosphates in yeast U6 snRNA specifically affect pre-mRNA splicing *in vitro*. *Nucleic Acids Res* **20:** 3659–3664

Fabrizio P, Dannenberg J, Dube P, Kastner B, Stark H, Urlaub H, Lührmann R (2009) The evolutionarily conserved core design of the catalytic activation step of the yeast spliceosome. *Mol Cell* **36:** 593–608

Fortner DM, Troy RG, Brow DA (1994) A stem/loop in U6 RNA defines a conformational switch required for pre-mRNA splicing. *Genes Dev* **8:** 221–233

Grainger RJ, Beggs JD (2005) Prp8 protein: at the heart of the spliceosome. *RNA* **11:** 533–557

Hilliker AK, Staley JP (2004) Multiple functions for the invariant AGC triad of U6 snRNA. *RNA* **10:** 921–928

Hogg R, McGrail JC, O'Keefe RT (2010) The function of the NineTeen Complex (NTC) in regulating spliceosome conformations and fidelity during pre-mRNA splicing. *Biochem Soc Trans* **38:** 1110–1115

Huppler A, Nikstad LJ, Allmann AM, Brow DA, Butcher SE (2002) Metal binding and base ionization in the U6 RNA intramolecular stem-loop structure. *Nat Struct Biol* **9:** 431–435

Jurica MS, Moore MJ (2003) Pre-mRNA splicing: awash in a sea of proteins. *Mol Cell* **12:** 5–14

Kandels-Lewis S, Séraphin B (1993) Involvement of U6 snRNA in 5′ splice site selection. *Science* **262:** 2035–2039

Keating KS, Toor N, Perlman PS, Pyle AM (2010) A structural analysis of the group II intron active site and implications for the spliceosome. *RNA* **16:** 1–9

Kim SH, Lin RJ (1996) Spliceosome activation by PRP2 ATPase prior to the first transesterification reaction of pre-mRNA splicing. *Mol Cell Biol* **16:** 6810–6819

Konarska MM, Query CC (2005) Insights into the mechanisms of splicing: more lessons from the ribosome. *Genes Dev* **19:** 2255–2260

Konarska MM, Vilardell J, Query CC (2006) Repositioning of the reaction intermediate within the catalytic center of the spliceosome. *Mol Cell* **21:** 543–553

Lesser CF, Guthrie C (1993) Mutations in U6 snRNA that alter splice site specificity: implications for the active site. *Science* **262:** 1982–1988

Madhani HD, Guthrie C (1992) A novel base-pairing interaction between U2 and U6 snRNAs suggests a mechanism for the catalytic activation of the spliceosome. *Cell* **71:** 803–817

Madhani HD, Guthrie C (1994) Dynamic RNA-RNA interactions in the spliceosome. *Annu Rev Genet* **28:** 1–26

McGrail JC, Krause A, O'Keefe RT (2009) The RNA binding protein Cwc2 interacts directly with the U6 snRNA to link the nineteen complex to the spliceosome during pre-mRNA splicing. *Nucleic Acids Res* **37:** 4205–4217

McManus CJ, Schwartz ML, Butcher SE, Brow DA (2007) A dynamic bulge in the U6 RNA internal stem-loop functions in spliceosome assembly and activation. *RNA* **13:** 2252–2265

Mefford MA, Staley JP (2009) Evidence that U2/U6 helix I promotes both catalytic steps of pre-mRNA splicing and rearranges in between these steps. *RNA* **15:** 1386–1397

Michel F, Costa M, Westhof E (2009) The ribozyme core of group II introns: a structure in want of partners. *Trends Biochem Sci* **34:** 189–199

Moine H, Ehresmann B, Ehresmann C, Romby P (1997) Probing RNA structure and function in solution. In: Simons RW, Grunberg-Manago M (eds). *RNA Structure and Function*. Cold Spring Harbor Laboratory Press: Cold Spring Harbor, NY. . pp 77–115

Nilsen TW (1998) RNA-RNA interactions in nuclear pre-mRNA splicing. In: Grundber-Manago M, Simons RW (eds). *RNA Structure and Function*. Cold Spring Harbor Laboratory Press: Cold Spring Harbor, NY, . pp 279–307

O'Keefe RT, Newman AJ (1998) Functional analysis of the U5 snRNA loop 1 in the second catalytic step of yeast pre-mRNA splicing. *EMBO J* **17:** 565–574

Ohi MD, Gould KL (2002) Characterization of interactions among the Cef1p-Prp19p-associated splicing complex. *RNA* **8:** 798–815

Pena V, Rozov A, Fabrizio P, Lührmann R, Wahl MC (2008) Structure and function of an RNase H domain at the heart of the spliceosome. *EMBO J* **27:** 2929–2940

Puig O, Caspary F, Rigaut G, Rutz B, Bouveret E, Bragado-Nilsson E, Wilm M, Séraphin B (2001) The tandem affinity purification (TAP) method: a general procedure of protein complex purification. *Methods* **24:** 218–229

Query CC, Konarska MM (2006) Splicing fidelity revisited. *Nat Struct Mol Biol* **13:** 472–474

Rhode BM, Hartmuth K, Westhof E, Lührmann R (2006) Proximity of conserved U6 and U2 snRNA elements to the 5′ splice site region in activated spliceosomes. *EMBO J* **25:** 2475–2486

Ritchie DB, Schellenberg MJ, Gesner EM, Raithatha SA, Stuart DT, Macmillan AM (2008) Structural elucidation of a PRP8 core domain from the heart of the spliceosome. *Nat Struct Mol Biol* **15:** 1199–1205

Shukla GC, Padgett RA (2002) A catalytically active group II intron domain 5 can function in the U12-dependent spliceosome. *Mol Cell* **9:** 1145–1150

Sontheimer EJ, Steitz JA (1993) The U5 and U6 small nuclear RNAs as active site components of the spliceosome. *Science* **262:** 1989–1996

Staley JP, Guthrie C (1998) Mechanical devices of the spliceosome: motors, clocks, springs, and things. *Cell* **92:** 315–326

Steitz TA, Steitz JA (1993) A general two-metal-ion mechanism for catalytic RNA. *Proc Natl Acad Sci USA* **90:** 6498–6502

Tarn WY, Hsu CH, Huang KT, Chen HR, Kao HY, Lee KR, Cheng SC (1994) Functional association of essential splicing factor(s) with PRP19 in a protein complex. *EMBO J* **13:** 2421–2431

Toor N, Keating KS, Fedorova O, Rajashankar K, Wang J, Pyle AM (2010) Tertiary architecture of the Oceanobacillus iheyensis group II intron. *RNA* **16:** 57–69

Toor N, Keating KS, Taylor SD, Pyle AM (2008) Crystal structure of a self-spliced group II intron. *Science* **320:** 77–82

Urlaub H, Hartmuth K, Lührmann R (2002) A two-tracked approach to analyze RNA-protein crosslinking sites in native, nonlabeled small nuclear ribonucleoprotein particles. *Methods* **26:** 170–181

Valadkhan S (2005) snRNAs as the catalysts of pre-mRNA splicing. *Curr Opin Chem Biol* **9:** 603–608

Valadkhan S, Manley JL (2002) Intrinsic metal binding by a spliceosomal RNA. *Nat Struct Biol* **9:** 498–499

Vander Kooi CW, Ren L, Xu P, Ohi MD, Gould KL, Chazin WJ (2010) The Prp19 WD40 domain contains a conserved protein interaction region essential for its function. *Structure* **18:** 584–593

Vidal VP, Verdone L, Mayes AE, Beggs JD (1999) Characterization of U6 snRNA-protein interactions. *RNA* **5:** 1470–1481

Villa T, Guthrie C (2005) The Isy1p component of the NineTeen Complex interacts with the ATPase Prp16p to regulate the fidelity of pre-mRNA splicing. *Genes Dev* **19:** 1894–1904

Warkocki Z, Odenwälder P, Schmitzová J, Platzmann F, Stark H, Urlaub H, Ficner R, Fabrizio P, Lührmann R (2009) Reconstitution of both steps of Saccharomyces cerevisiae splicing with purified spliceosomal components. *Nat Struct Mol Biol* **16:** 1237–1243

Will CL, Lührmann R (2011) Spliceosome structure and function. In: Gesteland RF, Cech TR, Atkins JF (eds). *RNA World*. Cold Spring Harbor Laboratory Press: Cold Spring Harbor, NY, . pp 181–203

Wu JA, Manley JL (1991) Base pairing between U2 and U6 snRNAs is necessary for splicing of a mammalian pre-mRNA. *Nature* **352:** 818–821

Xu D, Friesen JD (2001) Splicing factor Slt11p and its involvement in formation of U2/U6 Helix II in activation of the yeast spliceosome. *Mol Cell Biol* **21:** 1011–1023

Yang K, Zhang L, Xu T, Heroux A, Zhao R (2008) Crystal structure of the beta-finger domain of Prp8 reveals analogy to ribosomal proteins. *Proc Natl Acad Sci USA* **105:** 13817–13822

Yean SL, Wuenschell G, Termini J, Lin RJ (2000) Metal-ion coordination by U6 small nuclear RNA contributes to catalysis in the spliceosome. *Nature* **408:** 881–884

